Nucleic Acids Research, 2025, **53**, gkae1182
https://doi.org/10.1093/nar/gkae1182
Advance access publication date: 16 December 2024
Genomics

ZNF143 binds DNA and stimulates transcription initiation to activate and repress direct target genes

Jinhong Dong[1,†], Kizhakke Mattada Sathyan[1,†], Thomas G. Scott[2], Rudradeep Mukherjee[1] and Michael J. Guertin[1,3,*]

[1]Center for Cell Analysis and Modeling, University of Connecticut, 400 Farmington Ave, Farmington, Connecticut 06030, USA
[2]Department of Biochemistry and Molecular Genetics, University of Virginia, 1340 Jefferson Park Ave, Charlottesville, Virginia 22903, USA
[3]Department of Genetics and Genome Sciences, University of Connecticut, 400 Farmington Ave, Farmington, Connecticut 06030, USA

[*]To whom correspondence should be addressed. Tel: +1 607 542 9286; Email: guertin@uchc.edu
[†]These authors should be regarded as Joint First Authors.

Abstract

Transcription factors bind to sequence motifs and act as activators or repressors. Transcription factors interface with a constellation of accessory cofactors to regulate distinct mechanistic steps to regulate transcription. We rapidly degraded the essential and pervasively expressed transcription factor ZNF143 to determine its function in the transcription cycle. ZNF143 facilitates RNA polymerase initiation and activates gene expression. ZNF143 binds the promoter of nearly all its activated target genes. ZNF143 also binds near the site of genic transcription initiation to directly repress a subset of genes. Although ZNF143 stimulates initiation at ZNF143-repressed genes (i.e. those that increase transcription upon ZNF143 depletion), the molecular context of binding leads to *cis* repression. ZNF143 competes with other more efficient activators for promoter access, physically occludes transcription initiation sites and promoter-proximal sequence elements, and acts as a molecular roadblock to RNA polymerases during early elongation. The term *context specific* is often invoked to describe transcription factors that have both activation and repression functions. We define the context and molecular mechanisms of ZNF143-mediated *cis* activation and repression.

Graphical abstract

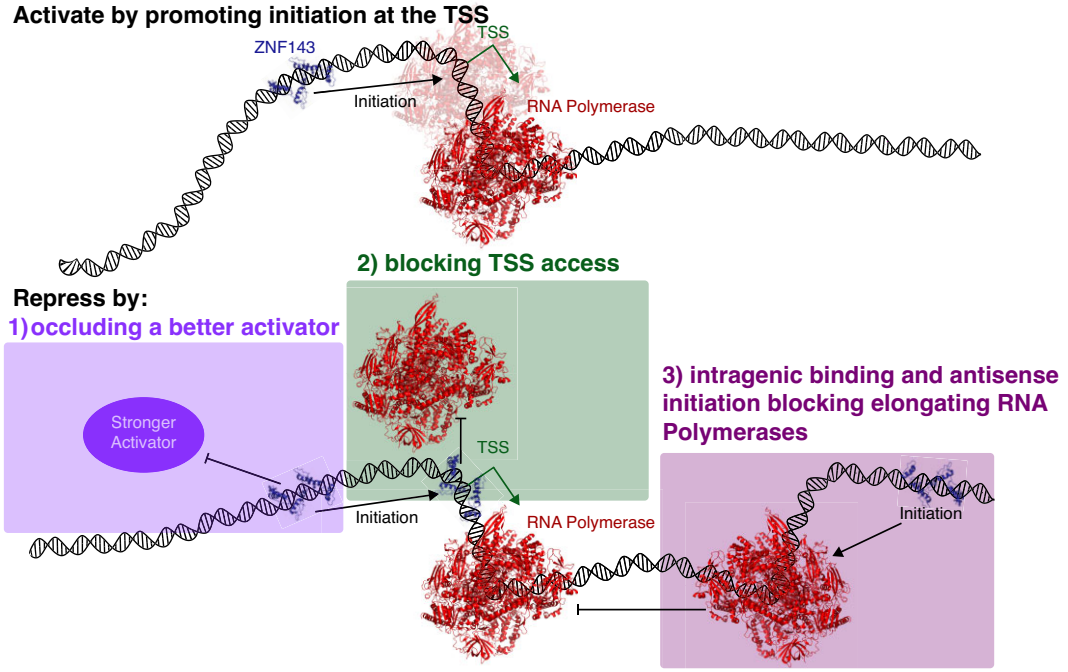

Received: May 29, 2024. **Revised:** September 30, 2024. **Editorial Decision:** November 1, 2024. **Accepted:** November 20, 2024

Introduction

Sequence-specific transcription factors bind directly to DNA and recruit cofactors and RNA polymerase to regulate gene expression throughout the lifetime of all organisms. Transcription factors specify tissue patterning throughout development and their function is necessary to maintain cellular and organismal homeostasis (1,2). Transcription factors are comprised of DNA binding domains that recognize degenerate sequence motifs and effector domains that interface with general transcription factors (GTF) and cofactors that specialize in regulatory roles such as chromatin remodeling, initiation, pause release and elongation. Just as cofactors and GTFs are specialists, transcription factors can specialize by predominantly regulating specific steps in transcription (3–5). Factors achieve this specificity by preferentially recruiting certain cofactors through their effector domains. We propose that it is critical to classify transcription factors by their molecular function, as opposed to broad activator and repressor classes, in order to understand the context specificity of gene regulation. For example, recruiting a transcription factor that specializes in RNA polymerase pause release to a gene may have little effect on transcription if redundant pause-release factors are already present; at this gene a factor that recruits components of the pre-initiation complex may cause potent activation. This work provides a framework for systematically determining the molecular functions of transcription factors by stimulating their rapid depletion and quantifying changes in RNA polymerase distribution at direct target genes in the minutes following transcription factor depletion.

Despite advances in understanding the mechanisms of transcription and developments in the systems biology of gene regulation field, accurately predicting direct target genes of transcription factors is a challenge. This struggle to predict target genes is in part because of the lack of reliable input data into predictive models. Researchers cannot experimentally identify a comprehensive set of primary response genes for the vast majority of transcription factors because they cannot rapidly induce or rapidly inhibit their activity. We know the most about transcription factors that are rapidly activated by acute environmental changes such as heat stress or nuclear receptor factors that are induced by addition of steroids (3,6–9). Many models rely on input data where a transcription factor is depleted chronically for days or the lifetime of a cell, so it is impossible to discriminate target genes from the complex cascade of transcription dysregulation that follows. However, recent development of rapidly inducible degron systems democratizes the study of transcription factors that are not easily activated or inhibited (10–12). Here, we C-terminally tagged all endogenous copies of the essential transcription factor ZNF143 with $FKBP^{F36V}$ in HEK-293T cells. We rapidly depleted ZNF143 by adding $dTAG^{V}$-1 to study its molecular function and define ZNF143's target genes.

The Xenopus homolog of ZNF143 was cloned and described three decades ago (13). This original report characterized the binding site and activator function of ZNF143 (contemporaneously termed Staf) using reporter assays (13). Subsequent transcriptional profiling upon chronic ZNF143 depletion identified many up regulated and down regulated genes (14); more genes were up regulated than down, and so the authors concluded that ZNF143 is primarily an activator while noting that ZNF143 may be involved in repression. Our results confirm that ZNF143 binds DNA within 500 bases of the transcription start site (TSS) and stimulates transcription initiation to activate genes. Furthermore, we define several molecular mechanisms through which a canonical activator can paradoxically retain its activator function while directly repressing target genes in *cis*. Although *cis* repression may only account for up to 30% of direct ZNF143-repressed targets, alternative mechanisms of immediate indirect repression, such as relieving competition for cofactors (15–17), may explain why additional genes are repressed indirectly.

While ZNF143's role in gene regulation was established nearly 30 years ago, many publications have since erroneously reported that ZNF143 has a prominent role in chromatin looping (18–23). However, two recent studies found that ZNF143 has no role in chromatin looping (24,25). These groups convincingly determine that the reason ZNF143 was ascribed a looping role is because a commonly used ZNF143 antibody crossreacts with the looping transcription factor CTCF (24,25). Herein we use rapid ZNF143 depletion and molecular genomics to determine the molecular mechanisms and context specificity of direct ZNF143-mediated activation and repression.

Materials and methods

HEK-293T culture and ZNF143-dTAG clone generation

HEK293T cells were cultured at 37°C with 5% carbon dioxide in DMEM media supplemented with 10% fetal bovine serum, 100 U/ml penicillin–streptomycin, 2.2 mM L-glutamine and 1 mM sodium pyruvate. We endogenously tagged ZNF143 at the C-terminus in HEK-293T cells as previously described (5,26). We targeted ZNF143 endogenously using CRISPR loaded with the following short guide RNA: GAGGATTAATCATCCAACCCTGG. We cleaved the hSpCas9 plasmid PX458 (Addgene #48138) with the enzyme BbsI, then annealed oligonucleotides 5′-CACCGAGGATTAATCATCCAACCC-3′ and 5′-AAACGGGTTGGATGATTAATCCTC-3′, and inserted the annealed product into the plasmid. We generated a linear homology-directed repair donor by amplifying the pCRISPITChv2-dTAG-Puro plasmid (Addgene #91796) with the primers in Table 1 (11). Following transfection of the donor DNA and Cas9/sgRNA plasmid into HEK-293T cells, cells were selected and cloned as described in (26). We selected cells in media with 1 μg/ml puromycin and confirmed successful integration by western blot as previously described (5). We performed sequencing to confirm that all ZNF143 alleles were tagged. All ZNF143 coding sequences are correct, but one tagged allele has a missense mutation at serine 68 in FKBP12, which converts the serine to an asparagine. Despite the mutation, ZNF143-dTAG efficiently degrades (Figure 1A and B). After obtaining a correctly-tagged clone we passaged cells thawed from frozen aliquots until the desired number of cells for each experiment was reached, and then treated with $dTAG^{V}$-1 and collected cells for ATAC-seq, PRO-seq and ChIP-seq.

Genome browser visualization

Genome browser (27) images were taken from the following track hub: http://guertinlab.cam.uchc.edu/znf143_hub/hub.txt.

Table 1. Homology directed repair primers

Primer	Sequence
Forward	5´-A*A*GAAGCCATCAGAATAGCGTCTAGAATCCAACA AGGAGAAACGCCAGGGCTTGACGACGGTGGCGGTGGCT CGGGC-3´
Reverse	5´-A*A*GACTCCTTCTGCTTTATTGCTCCATT GTTCTGAGGATTAATCATCCAATCAGGCACCGGGCTTG CGGGTC-3´

These primers amplify $FKBP^{F36V}$-2xHA-P2A-Puro with 50 bases of ZNF143 homology. The asterisks mark phosphorothioate bond modifications to minimize degradation.

ATAC-seq library preparation

We prepared ATAC-seq libraries as previously described (5,28). We treated cells with either Dimethylsulfoxide (DMSO) or $dTAG^V$-1 in DMSO for 30 min. After treatment, we aspirated the media and scraped the cells on ice and centrifuged them at 500 *g* for 5 min at 4°C. We resuspended cell pellets in lysis buffer (0.1% NP40, 0.1% Tween-20, 0.1% digitonin) made in cold resuspension buffer (10 mM Tris-HCl (pH 7.5), 10 mM NaCl, 3 mM $MgCl_2$ in water) and then incubated on ice for 3 min. We mixed lysates with wash buffer (0.1% Tween-20 in resuspension buffer) and centrifuged cells at 500 *g* for 10 min at 4°C. We resuspended the pellets in a transposition mixture (1 × Tagment DNA buffer, 0.1% ultrapure distilled water, 0.01% digitonin, 0.1% Tween-20 in phosphate-buffered saline (PBS) and added 2.5 µl of TDE1 Tn5 transposase (Illumina Tagment DNA TDE1 Enzyme and Buffer Kit). We incubated the transposition reaction at 37°C for 30 min. We isolated DNA from the reaction with the DNA Clean and Concentrator-5 kit. We added adapters and amplified DNA over eight cycles of polymerase chain reaction (PCR) using the NEBNext Ultra II kit. We purified and size selected the library by incubating samples with AMPure XP beads (1.8× buffer to sample ratio) and eluting with nuclease-free water.

PRO-seq library preparation

We prepared PRO-seq libraries as previously described (34,35). After 30 min of treatment with either 500 nM $dTAG^V$-1 or DMSO, we washed cells in ice cold PBS. We collected cells by adding buffer W [10 mM Tris-HCl (pH 7.5), 10 mM KCl, 250 mM sucrose, 5 mM $MgCl_2$, 1 mM EGTA, 10% glycerol, 0.5 mM Dithiothreitol, 0.004 U/ml SUPERaseIN RNase inhibitor and fresh protease inhibitors] and scraping the cells, followed by centrifugation at 500 *g* for 5 min and resuspension in buffer W. We added buffer P [10 mM Tris-HCl (pH 7.5), 10 mM KCl, 250 mM sucrose, 5 mM $MgCl_2$, 1 mM EGTA, 0.05% Tween-20, 0.1% NP40, 10% glycerol, 0.5 mM DTT, 0.004 U/ml SUPERaseIN RNase inhibitor and fresh protease inhibitors] for 5 min to permeabilize the cells. We centrifuged and resuspended the cells in buffer W twice before pelleting the cells again and resuspending in buffer F (50 mM Tris-HCl pH 8, 5 mM $MgCl_2$, 1.1 mM EDTA, 40% glycerol and 0.5 mM DTT). We snap froze aliquots in liquid nitrogen and kept them stored at −80°C. PRO-seq library prep was done in a method based on previously described protocols (34,36). After the run-on reaction, we added adapters that included a random eight base unique molecular identifier (UMI) on the 5′ end of adapter that is ligated to the 3′ end of the nascent RNA. We eluted and reverse transcribed the RNA and performed 10 cycles of PCR. We purified the PCR reactions with a MinElute PCR purification kit and did not perform size selection in an effort to preserve short nascent RNAs in our libraries. We sequenced the libraries using paired-end sequencing on a NextSeq 550.

PRO-seq analyses

Quality control and read alignment were performed as described previously (37). We used `cutadapt` v3.5 to remove adapters from our reads (38), and `fqdedup` v1.0.0 to deduplicate our libraries with the 3′ UMIs (https://github.com/guertinlab/fqdedup). We removed 8-mer UMIs and reverse complemented the reads with `FASTX-Toolkit` v0.0.14 (https://github.com/agordon/fastx_toolkit). We aligned to *hg38* with `bowtie2` v2.5.0 (29), sorted reads with `samtools` v1.16.1 (30), and used `seqOutBias` v1.4.0 (31) to convert reads to *bigWig* files. We used the PEPPRO guidelines (39) to assess purity of nascent RNA and run-on efficiency (Supplementary Figure S1). We used `primaryTranscriptAnnotation` v0.1.0 and `TSSinference` (https://github.com/guertinlab/TSSinference) to infer gene annotations from our PRO-seq data (40). We quantified nascent transcription by querying the *bigWig* files within the gene annotation coordinates with the `bigWig` v0.2.9 R package (https://github.com/andrelmartins/bigWig) and UCSC Genome Browser Utilities (`wigToBigWig` v2.9) (41). We found differentially expressed genes with `DESeq2` v1.38.3 (33). We normalized all replicates by read depth and combined replicates for each condition to obtain normalized intensities. We identified regions of bidirectional transcription with `dREG` v1.0 (42). We identified overrepresented motifs *de novo* in dREG-defined regions with `MEME` v5.4.1 (43). We modeled the rates of transcription initiation and pause release using a compartment model as previously described (44).

Compartment modeling

The compartment model was based on previous work from our lab (44) with some modifications. Briefly, we conceptualized transcription as RNA polymerases moving between compartments *p* (pause region) and *b* (the gene body) as defined by the TSS and transcription termination site (TTS) coordinates inferred from PRO-seq data by `primaryTranscriptAnnotation` v0.1.0 and `TSSinference` (https://github.com/guertinlab/TSSinference) (40). We defined rate constants for transcription initiation (k_{init}), promoter-proximal premature transcription termination (k_{pre}), pause release (k_{rel}) and elongation rate (k_{elong}) (Supplementary Figure S2).

We considered the measurements of read densities in pause windows and gene bodies to be at steady state. To determine the pause window for each gene, we searched within the first 200 bp downstream of the most prominent TSS and chose the 50 bp window with the maximum summed PRO-seq signal (*p*). The mean signal in the region starting 500 bp downstream of the pause window and ending at the TTS is *b*, the polymerase density within the gene body. We describe the change in *p* and *b* over time as:

$$\frac{dp}{dt} = k_{init} - (k_{pre} + k_{rel}) \cdot p \quad (1)$$

$$\frac{db}{dt} = k_{rel} \cdot p - k_{elong} \cdot b \quad (2)$$

The rates k_{elong} and k_{pre} were assumed to be unaffected by the treatment, whereas the values of k_{init} and k_{rel} may change.

We estimated parameters using the Levenberg–Marquardt algorithm provided by the COPASI engine (45) and estimated 700 parameter sets for each gene. The constraints on parameters (units in events/second) were as follows:

$$10^{-8} \leq k_{init}, k_{pre}, k_{rel} \leq 1$$

$$30 \leq k_{elong} \leq 60$$

These constraints were selected to encompass the range of previously published rates of transcription initiation, premature termination, pause release and transcription elongation (46–49).

ChIP and library preparation

We fixed cells with 1% formaldehyde for 10 min at 37°C and quenched them with 125 mM glycine for 10 min at 37°C. We then moved plates to ice and washed and scraped the cells into ice-cold PBS containing fresh protease inhibitors. We centrifuged cells in aliquots of 2×10^7 cells at 1500 *g* for 5 min, snap froze them in liquid nitrogen, and stored them at −80°C. After thawing the pellets, we lysed the cells in 1 ml lysis buffer with protease inhibitors [0.5% sodium dodecyl sulfate (SDS), 10 mM EDTA, 50 mM Tris-HCl (pH 8.0)] on ice for 10 min. Lysates were sonicated at 70% amplitude for 15 s on and 45 s off for four sets of 20-min cycles. We moved sonicated lysates to 1.5 ml tubes and clarified by centrifugation at 14 000 rpm for 10 min in 4°C. We diluted 50 µl of the supernatant into 760 µl ChIP Dilution Buffer [0.01% SDS, 1.1% Triton X-100, 1.2 mM EDTA, 167 mM NaCl, 16.6 mM Tris-HCl (pH 8.0), fresh protease inhibitors] for a total of 1×10^6 cells per replicate; 1 ml (4×10^6 cells) was aliquoted into each of 3 tubes with antibody (2 µg anti-HA Invitrogen #26183, 8 µg anti-SP1 Santa Cruz Biotechnology sc-17824 X, 7 µg anti-Nrf1 Invitrogen MA5-35366, or mock IP) and incubated with end-over-end rotation at 4°C overnight. We washed 80 µl Protein A/G Magnetic Beads (New England Biolabs) per sample with bead washing buffer (PBS with 0.1% BSA and 2 mM EDTA) prior to incubating with samples for 90 min with rotation at 4°C. After incubation the samples were washed once each with low salt immune complex buffer [0.1% SDS, 1% Triton X-100, 2 mM EDTA, 150 mM NaCl, 20 mM Tris HCl (pH 8.0)], high salt immune complex buffer [0.1% SDS, 1% Triton X-100, 2 mM EDTA, 500 mM NaCl, 20 mM Tris Hcl (pH 8.0)], LiCl immune complex buffer [0.25 M LiCl, 1% Igepal, 1% sodium deoxycholate, 1 mM EDTA, 10 mM Tris-HCl (pH 8.0)], and 1 × TE [10 mM Tris-HCl, 1 mM EDTA (pH 8.0)]. We eluted the immune complexes in elution buffer (1% SDS, 0.1 M sodium bicarbonate). We incubated each sample with 1µl RNase A for 10 min at 37°C. We digested the proteins by adding 5µl Proteinase K and incubating the samples in a 65°C water bath overnight. We purified DNA with a MinElute PCR purification kit, and prepared libraries with a NEBNext Ultra II Library Prep Kit.

ChIP-seq analyses

We removed adapters with `cutadapt` v3.5 (38) and aligned to the *hg38* genome assembly with `Bowtie2` v2.5.0 (29). We sorted aligned reads with `samtools` v1.16.1 and used `seqOutBias` v1.4.0 to generate *bigWig* files (30,31). All samples had aligned read depths above 10 million (Supplementary Figure S3). We called peaks with `MACS3` v3.0.0a6 (32). We quantified peak intensities by querying *bigWig* files in 400 base pair windows centered on peak summits and normalized the counts with `DESeq2` v1.38.3 (SP1 ChIP) or read depth normalization (ZNF143 ChIP) (33). We used the average normalized peak counts from the ZNF143 ChIP control samples to establish ZNF143 binding intensities and found differentially bound peaks of SP1 and Nrf1 before and after ZNF143 degradation with `DESeq2` v1.38.3 (33). We found *de novo* motifs with `MEME` v5.4.1 (43) and later `STREME` v5.4.1 (50) through rounds of iterative motif analysis whereby we used `MAST` v5.4.1 (51) to identify and remove the most common motifs for SP1 or ZNF143 until we stopped finding significant *de novo* motifs.

ATAC-seq analyses

We aligned raw sequence data to the *hg38* genome assembly with `Bowtie2` v2.5.0, converted to *BAM* format with `samtools` v1.16.1 and then to *bigWig* format with `seqOutBias` v1.4.0 (29–31). Peak calling with `MACS3` v3.0.0a6 (32) employed the following arguments: `-q 0.01 –keep-dup all –nomodel –shift -100 –extsize 200`. We counted reads in peaks with the `bigWig` v0.2.9 R package (https://github.com/andrelmartins/bigWig) and called differentially accessible regions with `DESeq2` v1.38.3 (33). We calculated fraction of reads in peaks and aligned read depth to assess quality of libraries (Supplementary Figure S4).

Results

ZNF143 is not detected on DNA after 30 min of degradation

To determine the molecular function of ZNF143, we engineered HEK-293T cells to express all alleles of ZNF143 tagged with a C-terminal inducible dTAG degron system, facilitating rapid and complete protein degradation (11). Endogenous tagging of ZNF143 causes a modest decrease in protein levels (Figure 1A, lanes 1 and 2, and Supplementary Figure S5A). Quantitative western blots indicate that <10% of ZNF143 remains after 15 min of $dTAG^V$-1 treatment and ZNF143 is not detected at 30–90 min after induced degradation. We profiled ZNF143 binding genome-wide by ChIP-seq before and after 30 min of degradation to quantify depletion on chromatin. On the same scale, ZNF143 is not detectable after 30 min of degradation (Figure 1B), but digital over-exposure of the heatmaps indicates that <5% of the original ZNF143 signal is detected on DNA (Supplementary Figure S5B). This cell line represents a powerful resource for investigating the molecular functions of ZNF143 and directly identifying ZNF143 target genes.

ZNF143 binds a degenerate 29 base motif at each binding site in the genome

Next, we conducted iterative and exhaustive motif analysis of ZNF143 ChIP-seq peaks to systematically identify and characterize the diverse sequence motifs that ZNF143 binds in the genome. We performed *de novo* motif analysis within the 4682 ZNF143 ChIP-seq peaks and identified a canonical ZNF143 sequence motif within 58% peaks (Figure 1C). ZNF143's seven zinc fingers are known to bind a wider region (23), so we performed the same analysis on remaining peaks that lack the first identified motif. We found a second ZNF143 motif variant and two more iterations of this process identified

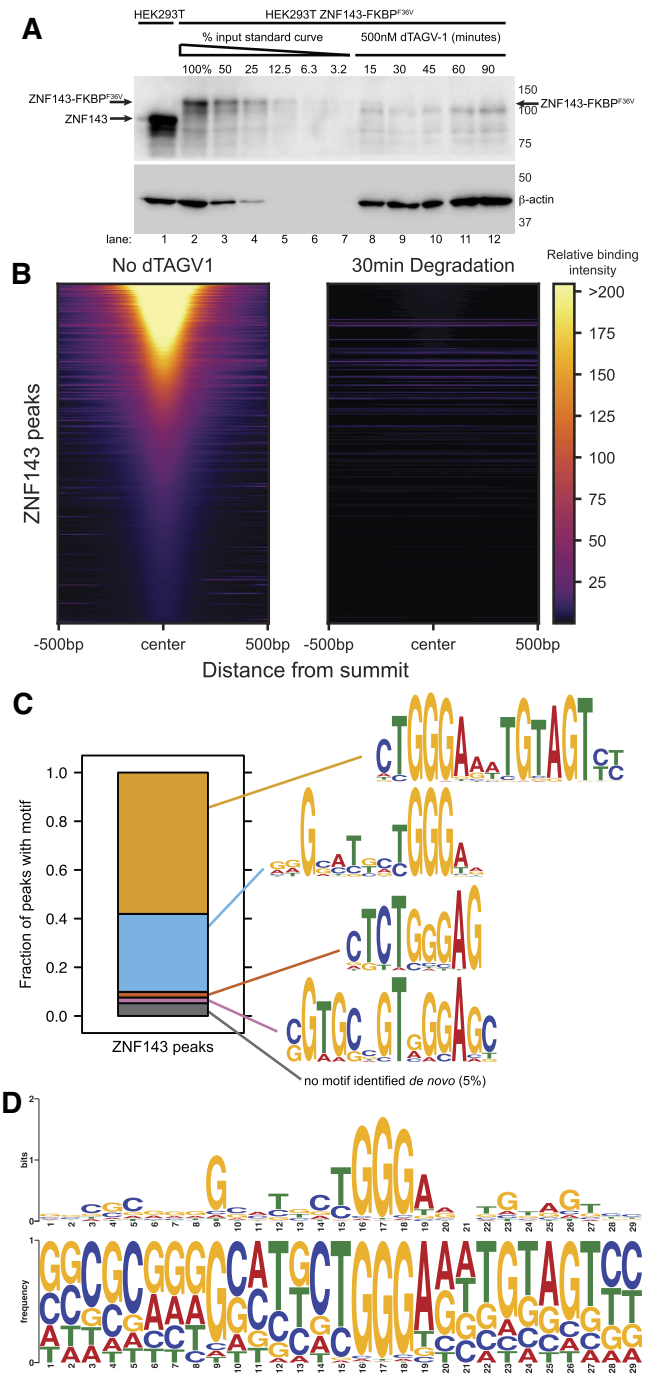

Figure 1. ZNF143 is degraded and not detected on chromatin within 30 min of dTAG^{V}-1-induced degradation. (**A**) Quantitative western blots indicate that FKBPdegron^{F36V}-tagged ZNF143 (lane 2) is expressed at 50% of untagged ZNF143 (lane 1). Lanes 2–7 are dilutions of the untreated and tagged cell line. Lanes 8–12 are a time series of degradation. Note that the arrow represents ZNF143 and there is a nonspecific band that is unchanged directly below the arrow. (**B**) A heatmap of all 4682 ZNF143 ChIP-seq peaks indicates that ZNF143 is not detected on chromatin after 30 min of degradation. The color scale represents relative binding intensities of ZNF143 as determined by read depth-normalized ChIP-seq data. (**C**) Iterative *de novo* motif analysis identified four ZNF143 motifs that are anchored on a central TGGGA sequence. A total of 95% of ZNF143 peaks have at least one motif that conforms to a *de novo*-identified motif with a *P*-value of 0.0005 of lower. (**D**) The 29 mer seqLogo represents the average ZNF143 binding site, where substantial degeneracy is tolerated outside the core TGGGA postion. The first seqLogo has information content (in bits) as the y-axis, whereas the second seqLogo shows the individual ACGT frequency at each position.

other ZNF143 motifs (Figure 1C). A total of 95% of the peaks had a *de novo*-identified motif that was clearly a ZNF143 motif variant (Figure 1C). These findings demonstrate ZNF143's flexibility in binding; it can accommodate a wide range of sequences beyond the core **TGGGA** sequence that is recognized by zinc fingers 5 and 6 (23). By anchoring the analysis on this core sequence, we calculated the average frequency of each nucleotide (A, C, G, T) within a 100-base range, highlighting how ZNF143's binding preferences extend into the surrounding genomic landscape. The nucleotide frequencies stabilize outside a 29-mer core ZNF143 motif. This 29-mer core is similar to the biochemically determined 27-mer ZNF143 core motif found previously (23). We generated a composite motif using the frequencies in this window (Figure 1D). We did not identify a motif *de novo* in 5% of binding sites; however, these peaks remain sensitive to ZNF143 depletion and retain potential functionality. Low-affinity binding sites of transcription factors, which do not strictly conform to a consensus motif, are increasingly recognized as having a critical role in gene regulation and development (53,54). We determined the precise ZNF143 binding positions within each ChIP-seq peak by assigning the motif with the lowest *P*-value in the peak as the inferred 29 base binding site (Supplementary Figure S5C). All subsequent references and analyses concerning ZNF143 binding focus on the 29-mer ZNF143 recognition sequences within the ChIP-seq peaks. These analyses confirm the DNA-binding function of ZNF143 and indicate that ZNF143 binds a sequence-degenerate 29 base wide motif within chromatin.

ZNF143 maintains chromatin accessibility at a minority of binding sites

To investigate the impact of ZNF143 on chromatin accessibility, we conducted ATAC-seq analysis before and after 30 min of ZNF143 depletion. Fewer than 700 ATAC-seq peaks significantly (False Discovery Rate < 0.1) change accessibility after 30 min of ZNF143 depletion (Figure 2A). Over 99% of the significantly changed ATAC peaks decrease accessibility and 92% of the decreased accessibility peaks overlap ZNF143 binding sites (Figure 2B&C). Although the vast majority of decreased ATAC peaks are directly regulated by ZNF143 binding, the inverse is not true. Only a minority (13%; 620/4682) of ZNF143 ChIP-seq peaks show significantly reduced chromatin accessibility upon ZNF143 ablation from chromatin. These results underscore that while ZNF143 maintains open chromatin at certain loci, its influence is not uniform across all binding sites, suggesting that regulating chromatin structure is not its primary function.

ZNF143 is an activator that predominantly regulates transcription initiation

We performed nascent RNA profiling (PRO-seq) after 30 min of ZNF143 depletion to identify direct ZNF143 target genes (55). Hundreds of genes increase (*up*) and decrease (*down*) transcription after 30 min of ZNF143 depletion (Figure 3A). Although the expression of primary response genes goes in both directions, this does not necessarily mean that ZNF143 functions as an activator and a repressor. The transcription factors that we know most about are rapidly inducible, such as heat shock factor and nuclear hormone receptors such as the estrogen, androgen and glucocorticoid receptors. Although genes are activated and repressed in the minutes following the activation of these transcription factors, only the activated genes are closer to the respective binding sites of the factor

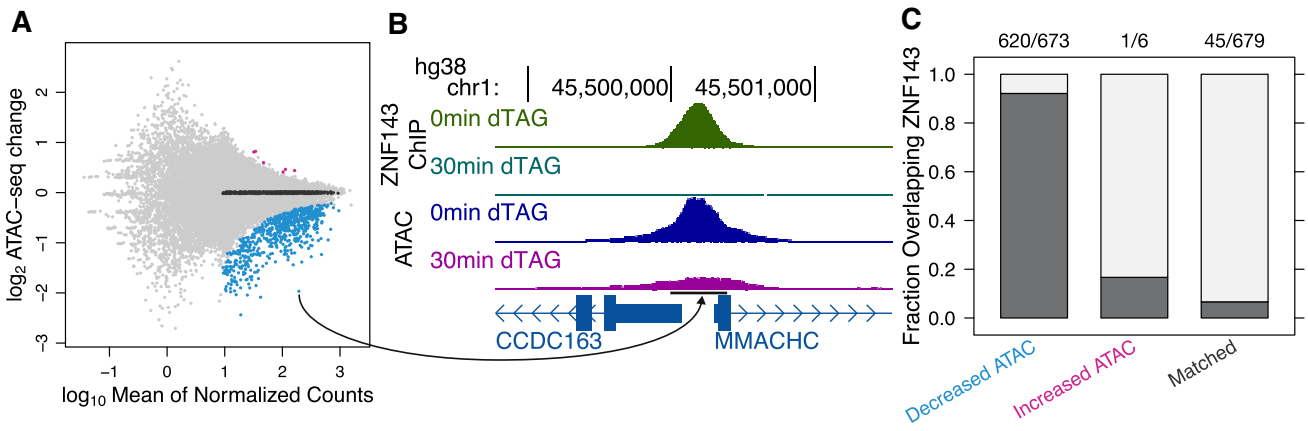

Figure 2. ZNF143 degradation leads to a decrease in chromatin accessibility. (**A**) The MA plot for the ATAC-seq peaks show that only six ATAC-seq peaks increase chromatin accessibility after 30 min of ZNF143 depletion and 673 peaks decrease accessibility (FDR < 0.1). Pink indicates increased ATAC peaks, and blue indicates decreased peaks. Dark gray dots are peaks that did not change accessibility significantly but are matched to increased and decreased peaks on mean normalized peak intensity using the R package `MatchIt` (52). (**B**) An example ATAC-seq peak in the CCDC163 promoter decreases accessibility and overlaps a ZNF143 binding site. (**C**) A total of 95% of ATAC peaks with reduced accessibility overlap with ZNF143 binding sites. Although only a subset of ZNF143 binding events is linked to changes in chromatin accessibility, when ZNF143 is actively influencing chromatin, it primarily functions to maintain chromatin accessibility.

(3,15,44,56–58). The repressed genes are no closer to the factor binding sites than unchanged control genes, so only the activated genes are considered direct *cis* targets of these transcription factors. We performed these same gene class/peak proximity analyses for the ZNF143 regulated genes and unchanged genes that are matched for nascent transcription levels (Figure 3B). Nearly all the *down* genes have their maximum TSS within 500 bases of a ZNF143 binding site (Figure 3B) and the vast majority of ZNF143 binding sites are in the upstream promoter region (Figure 3C). Unlike the heat shock and hormone response systems, the opposing *up* gene class is enriched for ZNF143 binding within 500 bases of an *up* gene maximum TSS (Figure 3B), although ZNF143 binding is not limited to the promoter region (Figure 3C). These results reveal that the predominant function of ZNF143 is to activate transcription proximally. Next we will focus on determining the molecular mechanism of ZNF143-mediated activation.

The transcription cycle includes many steps including chromatin decondensation, RNA polymerase recruitment/initiation, promoter-proximal pause termination or release, and elongation (59,60). We quantified the change in PRO-seq density within the 5′ pause region and gene bodies of *down* genes and incorporated these values into a compartment model (Supplementary Figure S2) to determine whether ZNF143 predominately regulates initiation or pause release. Our modeling analysis indicates that a decrease in initiation rate at every *down* gene with ZNF143 binding within the 500 base promoter best explains the redistribution of RNA polymerase in the pause and gene body regions upon ZNF143 depletion (Figure 3D). In contrast, pause release rates change in both directions (Figure 3D). Compartment modeling of changes in PRO-seq signal cannot distinguish between decreasing initiation and increasing premature pause termination because these are directly opposing rate constants (Supplementary Figure S2).

To determine whether ZNF143 regulates initiation/ recruitment versus premature pause termination we sought to determine whether ZNF143 affects TSS usage. Our rationale is that if ZNF143 regulates initiation, then the predominant TSS would change upon ZNF143 depletion. Previous work showed that rapid depletion of the initiation factor TATA-binding protein causes changes in TSS usage (61). The 5′ end of PRO-seq reads accumulate at a gene's TSS and we inferred the most prominent TSS (max TSS) before and after 30 min of ZNF143 degradation from 5′ read pileups. We focused this analysis exclusively on *down* genes with ZNF143 binding in the 500 base promoter region. *Down* genes with promoter-bound ZNF143 shift their most prominent TSS at twice the rate compared to a control set of genes matched for TSS signal intensity (Figure 3E). For example, after ZNF143 degradation *ZNF30*'s max TSS shifts from 159 to 18 bases away from ZNF143's binding site (Figure 3E). This suggests that ZNF143's close proximity inhibits initiation at the alternative dTAG TSS. TSSs within the human genome are not focused at a single position, but occur in windows and genes can contain multiple TSS windows (62). The observed changes in the most prominent TSS could occur because signal decreases at the control TSS and an alternative less prominent TSS does not change intensity. However, we observe a coupled decrease in signal at the control TSS and an increase in signal at the ZNF143-depleted TSS (Figure 3F). This pattern suggests that not only does ZNF143 regulate transcription initiation as opposed to premature termination, but the redistribution of TSS signal suggests that ZNF143 competes with other transcription factors for RNA polymerase and/or initiation machinery. The role of ZNF143 stimulating initiation is consistent with the chromatin accessibility data from Figure 2. Although chromatin structure is influenced directly by the recruitment of chromatin remodelers and histone-modifying enzymes, the recruitment of RNA polymerase or initiation factors can also deplete nucleosomes, thereby altering the chromatin landscape.

ZNF143 directly represses genes by binding directly over TSSs

The canonical molecular functions of ZNF143 are succinctly described as DNA binding and stimulation of transcription initiation. However, it is not immediately clear how these functions lead to the direct *cis* repression of ZNF143 target

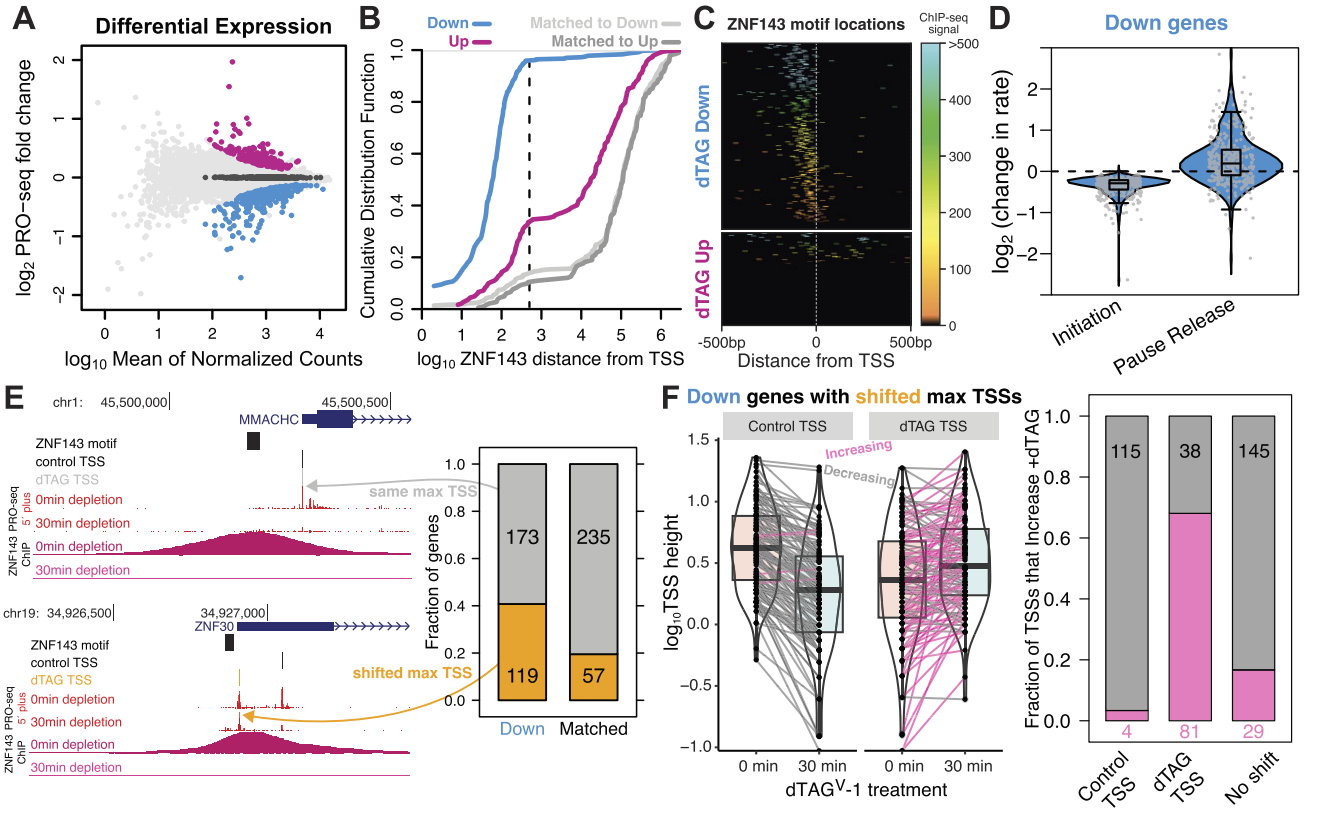

Figure 3. ZNF143 binds in promoters to directly regulate transcription initiation. (**A**) The nascent transcriptomics MA plot of 13 276 genes shows 182 genes that increase transcription (*up*, pink) and 365 genes that decrease (*down*, blue) after 30 min of ZNF143 degradation (FDR < 0.1). The dark gray dots represent genes that do not change expression after ZNF143 degradation but are matched to the mean normalized gene expression of the differentially expressed genes. (**B**) A total of 95% of *down* genes are within 500 bases of a ZNF143 binding site. The *up* genes are also significantly closer to ZNF143 binding sites compared to genes that are matched for expression level. The light and dark gray traces indicate the distances from unchanged genes' TSSs to the nearest ZNF143 binding site for matched genes. (**C**) *Down* genes have ZNF143 binding in the promoter; *up* genes have no clear pattern of ZNF143 distribution and 66% have no local ZNF143 binding. The color scale represents the mean control sample ChIP-seq signal at each of these motifs, which was normalized by read depth. (**D**) Compartment modeling indicates that ZNF143 regulates initiation and not pause release at direct *down* target genes. Each point is a *down* gene and the y-axis values are the changes in rates that most likely explain the data. (**E**) We inferred the locations of the predominant maximum TSS (max TSS) of each gene from normalized PRO-seq data for the control and dTAG conditions separately. The locations of the max TSS of direct *down* target genes tend to change upon ZNF143 degradation. (**F**) We quantified the level of TSS usage with TSS height, which refers to the mean normalized PRO-seq signal at that specific TSS in either the control or dTAG condition. The paired box-and-whisker/violin plots show that, for the *down* genes with shifted max TSSs, a decrease in the control max TSS height is frequently accompanied by an increase at the dTAG max TSS height. The bar charts show the fraction of max TSSs that increase in height after ZNF143 degradation for the control and dTAG max TSSs separately, as well as the change in TSS height for genes that did not have a shifted max TSS after ZNF143 degradation.

genes observed in Figure 3B. ZNF143 binds both upstream and downstream of *up* genes at comparable frequencies (Figure 3C), but it directly binds over the TSS of five genes (Figure 4A and B). ZNF143 exhibits stronger binding over the TSS of four out of these five genes compared to matched and *down* genes with TSS-bound ZNF143 (Figure 4B). These observations support a model in which ZNF143 binding directly over the TSS competes with RNA polymerase for access to the initiator sequence. The distribution of 5′ PRO-seq reads remains consistent with or without ZNF143 depletion at the one *up* gene, *FIS1*, that exhibits weak ZNF143 binding over the TSS (Figure 4C). However, a closer inspection of this gene reveals that the most prominent TSS changes upon ZNF143 depletion and 5′ PRO-seq signal substantially increases at this new maximum TSS (Figure 4D). A much stronger ZNF143 binding site is located directly downstream of this *FIS1* TSS-isoform (Figure 4D). This observation suggests an independent repressive mechanism, where ZNF143 binding directly downstream of a TSS acts as a molecular roadblock, which will inhibit RNA polymerase from progressing into the gene body and effectively repress transcription.

ZNF143 directly represses genes by acting as a molecular roadblock immediately downstream of TSSs

FIS1 was not initially classified as a ZNF143-downstream gene because we inferred a single isoform of each primary transcript using the control data (40). We then extended our analysis to the 28 *up* genes with ZNF143 binding within 500 bases downstream of their control TSSs (Figure 4E and F). These 28 genes have strong ZNF143 binding downstream of their start sites compared to matched and *down* genes with downstream ZNF143 peaks (Figure 4F). These results are consistent with a molecular roadblock model, whereby strong transcription factor binding can inhibit RNA polymerase during early elongation when it is accelerating and more vulnerable to pausing, backtracking and disassociation. Beyond ZNF143's role in DNA binding, we have established that it

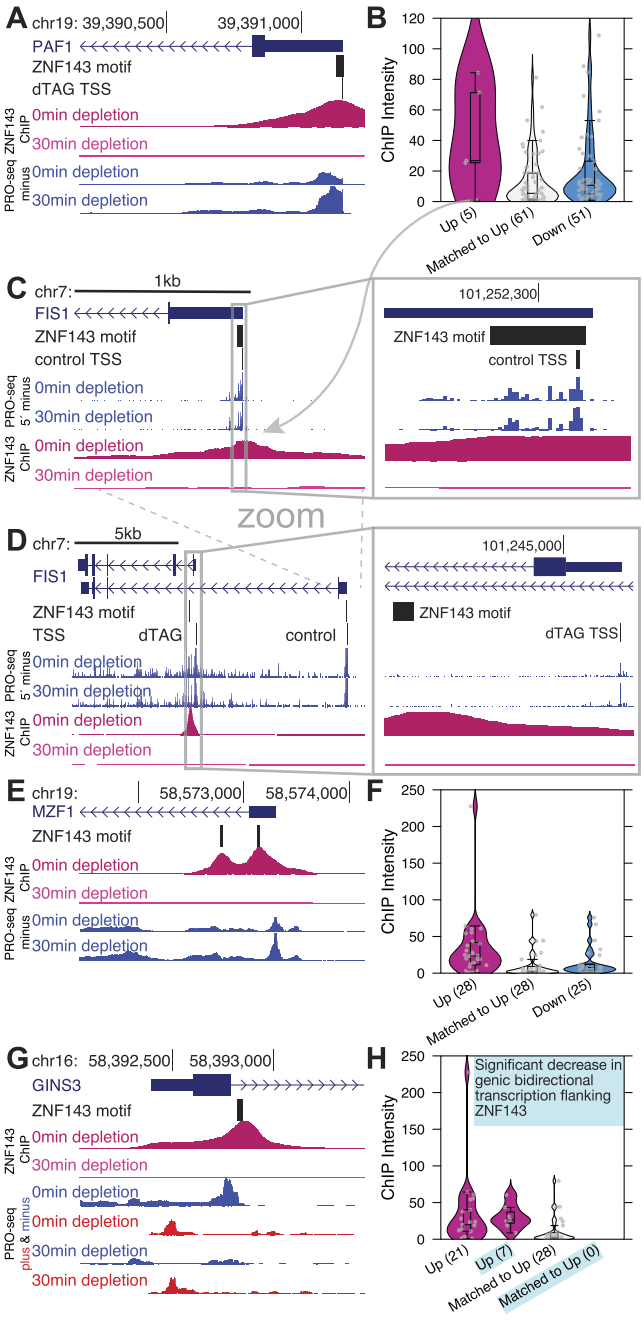

Figure 4. ZNF143 occludes sites of initiation and acts as a molecular roadblock to directly repress genes in *cis*. (**A**) ZNF143 binds a 29bp motif that spans *PAF1*'s TSS. *PAF1* transcription increases upon ZNF143 depletion. (**B**) Each point with the violin plots is a bound ZNF143 motif that spans a max TSS of the respective class. ZNF143 binds strongly over the TSS of 4/5 genes that increase transcription upon ZNF143 depletion. (**C**) *FIS1* is the *up* gene from panel (B) with weak TSS binding of ZNF143 and no discernible changes in TSS usage occur upon depletion, as measured by PRO-seq 5′ end pile ups. (**D**) ZNF143 binds directly downstream from the TSS of a different isoform of *FIS1*. This *FIS1* isoform becomes the most prominent *FIS1* TSS upon ZNF143 degradation. A zoomed in view of main dTAG TSS is visualized in the right panel. (**E, F**) ZNF143 degradation from strong binding sites directly downstream of TSSs is associated with *up* genes. (**G, H**) Genic bidirectional transcription at ZNF143 binding sites downstream of *up* genes significantly decreases at 7/28 *up* genes.

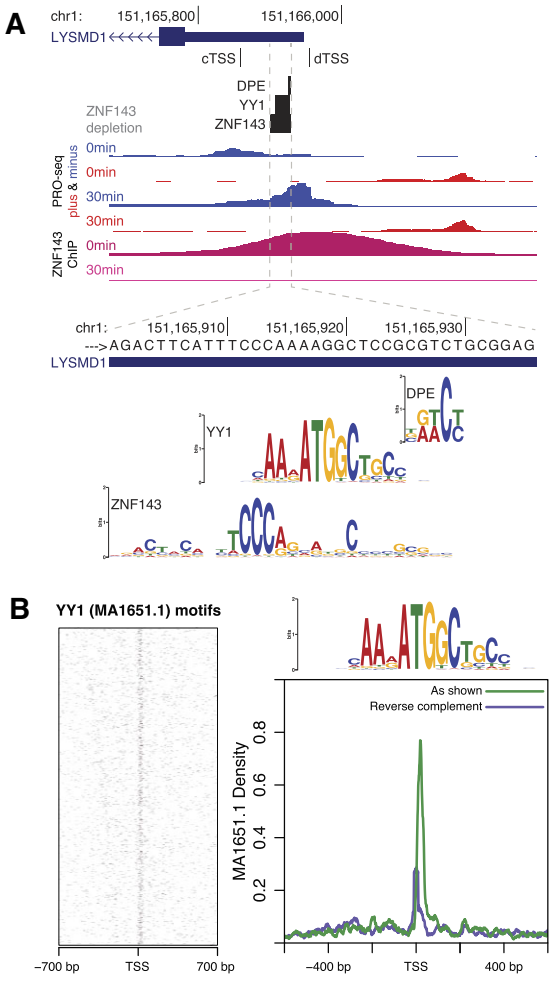

Figure 5. ZNF143 occludes downstream sequence elements to repress transcription. (**A**) ZNF143 depletion reveals an accessible YY1 motif and DPE that allows usage of a TSS that is 28 bases upstream of the ZNF143 binding site in the *LYSMD1* promoter (cTSS, control max TSS position; dTSS, dTAG max TSS position). (**B**) YY1's motif (MA1651.1) is enriched directly downstream of TSSs.

also stimulates initiation. Importantly, RNA polymerase initiates transcription at bidirectional regions across the genome, not solely at genic TSSs (63,64). Bidirectional transcription (42,65), especially an RNA polymerase colliding head on with an elongating RNA polymerase or paused RNA polymerase, could also act to repress transcription. We find that 7 out of these 28 downstream ZNF143-binding genes have significantly reduced bidirectional transcription after ZNF143 depletion (Figure 4G and H). This evidence supports the hypothesis that ZNF143 not only activates but may also repress transcription by promoting RNA polymerase initiation, highlighting the importance of proposing specific mechanisms when claiming transcription factors have dual activation/repression functions.

ZNF143 occludes downstream sequence elements to repress transcription

ZNF143 binds to the promoters of three *up* genes that have an upstream shift in their TSS after ZNF143 depletion (Figure 5A and Supplementary Figure S6). We hypothesized that ZNF143 binding occludes a downstream sequence motif that

contributes to initiation. The downstream promoter element (DPE) located +28 to +32 downstream of TSSs was the first downstream element shown to contribute to initiation by interacting with TFIID (66). ZNF143 blocks a DPE that is located at positions +27 to +31 within the *LYSMD1* gene. Additionally, YY1, an initiation factor (67,68), has a binding motif that is commonly found directly downstream of TSSs and between +100 and +300 positions downstream (69,70) (Figure 5B). ZNF143 binds upstream of *LYSMD1*, *GMPR2*, and *ZNF583*, and upon ZNF143 depletion, a YY1 motif becomes accessible at each of these genes (Figure 5A and Supplementary Figure S6). YY1 binding at the exposed site may facilitate efficient initiation at the upstream TSS. This YY1 occlusion mechanism may be acting simultaneously as a roadblock and/or directing genic bidirectional transcription for the upstream dTAG TSS (Supplementary Figure S6). These three *up* genes are unique because ZNF143 is promoter-bound and ZNF143 depletion causes an upstream TSS shift. This mechanism cannot explain repression at *up* genes with promoter-bound ZNF143 and no upstream TSS shift.

SP1 and Nrf1 redistribute to ZNF143 binding sites to stimulate initiation

ZNF143 bound the promoters of 25 *up* genes with distances and intensities comparable to those of *down* genes and no TSS shift upstream of ZNF143's binding site (Figure 3C). Given the limited number of *up* genes, we catalogued all bidirectionally transcribed putative regulatory elements across the genome and analyzed transcriptional changes in these regions after ZNF143 depletion (33,42) (Supplementary Figure S7A and B). We then carried out *de novo* motif discovery within the bidirectionally transcribed regions of both *down* and *up* classes. As anticipated, the ZNF143 motif was prevalent in the *down* class; however, its presence in the *up* class was unexpected (Supplementary Figure S7B). Additionally, the SP transcription factor family DNA motif was identified *de novo* in the *up* class (Supplementary Figure S7B). A total of 99 bidirectional *up* regions have both ZNF143 ChIP peaks and ZNF143 motifs, with 19 of the ZNF143 motifs overlapping SP motifs (Supplementary Figure S7C and D). We performed SP1 ChIP-seq before and after 30 min of ZNF143 depletion to address the possibility that SP1 is redistributing to these sites when ZNF143 vacates. Each of the these 19 regions overlapped an SP1 ChIP-seq peak and 13 of the peaks increased SP1 intensity upon ZNF143 depletion (Supplementary Figure S7E). SP1 also regulates initiation (44,72), so these results are consistent with a model whereby a canonical activator can repress a gene if it competes with a more potent activator for the same stretch of DNA. SP1 is clearly not replacing ZNF143 at all nineteen sites, but recall that ZNF143 binds a 29 base region and the ZNF143 motif may be overlapping the motifs for other initiation factors.

SP1 motifs were among the first promoter sequence elements to be identified as regulatory (73) and SP1 has had a defined role in initiation for 30 years (72). Recent studies have further refined SP motifs as defining elements of promoter architecture in the genome (69,70,74). Motifs recognized by paralogs of ZNF143, along with Nrf1, ETS, NFY, CREB/ATF (bZIP) and SP/KLF factors, are considered critical in dictating promoter structure and initiating transcription (69,70,74). The sequence-specific transcription factors that bind these motifs may be a class of sequence-specific transcription factors that recruit the initiation machinery and RNA polymerase. Our findings confirm the enrichment of these motifs within bidirectional promoters across the human genome (Figure 6A and Supplementary Figure S7). We searched for the motifs of these sequence-specific initiation transcription factors within the 29-mer ZNF143 motif of these 25 genes with promoter-bound ZNF143. At least one of the bZIP, SP/KLF, ETS and Nrf1 motifs overlapped the ZNF143 motif in all genes except *TSNAXIP1* (Supplementary Figure S8A). We also observe the same overlap of ZNF143 and Nrf1/ETS/SP motifs at bidirectionally transcribed regions from Supplementary Figure S7D (Supplementary Figure S8A).

We propose that other activating factors replace ZNF143 at these promoters when ZNF143 is depleted. To test this hypothesis, we performed Nrf1 ChIP-seq before and after ZNF143 depletion and we analyzed differential SP1 and Nrf1 binding at the SP1/ZNF143 and Nrf1/ZNF143 overlaps in *up* gene promoters. Sixteen *up* genes with ZNF143 in the promoter have an overlapping SP motif within an SP1 ChIP-seq peak and 10 of the 16 have an increase in SP1 ChIP signal after ZNF143 depletion (Figure 6B and C, and Supplementary Figure S8B). The promoters of *ZNF688*, *UTP3* and *PYCR2* exhibit a statistically significantly (FDR < 0.01) increase in SP1 signal upon ZNF143 depletion (Figure 6C). Fifteen *up* gene promoters with overlapping Nrf1/ZNF143 motifs also overlap Nrf1 ChIP-seq peaks (Figure 6D and E, and Supplementary Figure S8C). *ZNF324B* and *LRRC45* had significantly increased Nrf1 binding after ZNF143 depletion (FDR < 0.01, Figure 6E). These results suggest that a canonical activator may repress genes by competing for DNA binding with a more potent activator. However, we appreciate that the molecular calculus for such a mechanism is complex. For instance, a very strong activator might have a brief residency time on DNA, making its overall contribution minimal, while a modest activator could have more stable DNA binding and effectively stimulate transcription. Given that each promoter has a unique sequence context, predicting transcriptional outcomes solely based on sequence is challenging. To fully understand the competitive interactions between two transcription factors targeting the same DNA region, one must consider: (i) their relative binding efficiencies and residency times within specific chromatin contexts; (ii) the transcription cycle stages each factor influences; (iii) the relative activation potency of each factor; and (iv) which step(s) in the transcription cycle limit transcriptional output of the target gene.

Discussion

When discussing the context-specific dual roles of transcription factors as both activators and repressors, it is crucial to propose an underlying mechanism (Figure 7). The most well characterized example of dual activator/repressor function in gene regulation is that of the λ repressor. The λ repressor is an activator that interacts with the bacterial RNA polymerase to stimulate initiation, but it was named *repressor* because it represses transcription of the lytic genes, which account for nearly all the phage genes. The λ repressor binds to a precise position in its own promoter to stimulate RNA polymerase initiation and activate the gene encoding itself (75). This same binding event blocks RNA polymerase from accessing and initiating transcription of lytic genes (75–77). The molecular functions of both λ repressor and ZNF143 are to bind DNA and stimulate initiation. Binding of ZNF143 to DNA is neces-

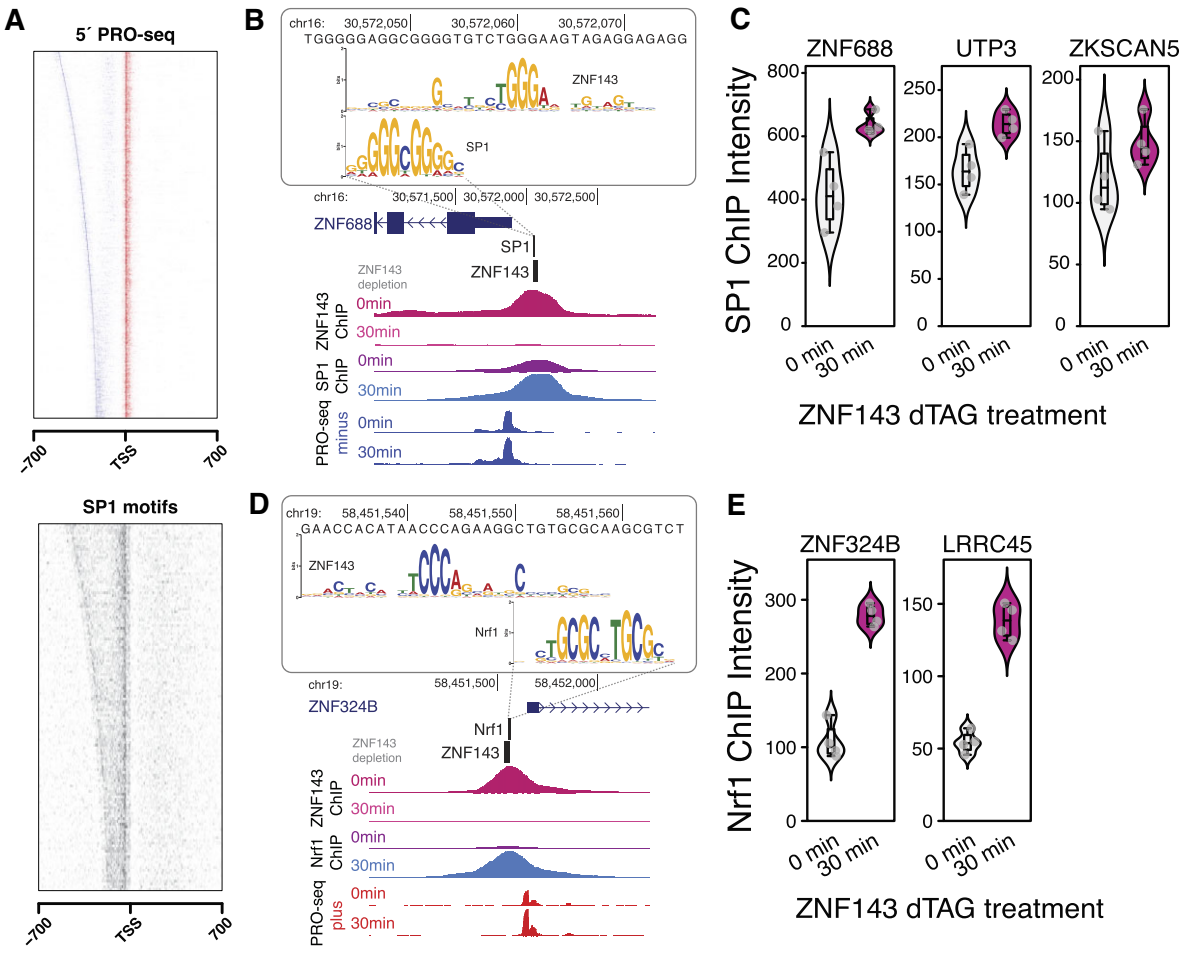

Figure 6. ZNF143 represses nascent transcription by competing with SP1 and Nrf1 for promoter binding. (**A**) We identified promoter regions within sense and divergent TSSs called from pileups of the 5′ ends of PRO-seq reads. SP motifs identified by FIMO (71) are enriched in regions between bidirectional start sites. (**B**) After ZNF143 degradation, *ZNF688* transcription increases and SP1 ChIP-seq signal overlapping ZNF143 increases significantly. Sequence logos for ZNF143 and SP1 demonstrate the overlapping binding sites of these factors. The *ZNF688* 5′ untranslated region annotation is extended to the TSS inferred from our PRO-seq data because this position also aligns with the human expressed sequence tag HY111461. (**C**) SP1 ChIP-seq signal overlapping ZNF143 increases significantly (FDR < 0.01) after ZNF143 degradation and increased gene expression for genes *ZNF688, UTP3* and *ZKSCAN5*. (**D**) After ZNF143 degradation, *ZNF324B* transcription increases and Nrf1 ChIP-seq signal overlapping ZNF143 increases significantly. Sequence logos for ZNF143 and Nrf1 illustrate the overlapping binding sites of these factors. (**E**) Nrf1 ChIP-seq signal overlapping ZNF143 increases significantly (FDR < 0.01) after ZNF143 degradation in the promoters of *ZNF324B* and *LRRC45*.

sary to stimulate initiation; like λ repressor, ZNF143 typically binds upstream of a initiation site to activate transcription. Binding in a promoter and stimulating initiation may result in repression if ZNF143 displaces a more potent stimulator of initiation. Binding over an initiator sequence or within a gene body can cause repression via multiple described mechanisms. While ZNF143 can both activate and repress genes, its molecular functions of DNA binding and promoting initiation remain constant.

Many transcription factors are described as having both activator and repressor activities and *context specificity* is often vaguely invoked as the explanation. There are conflicting reports on whether MYC acts as an activator at specific genes or a direct repressor at some genes (78–82). The acute depletion of an auxin inducible degron tagged MYC within 30 min, coupled with nascent RNA sequencing, allowed for the identification of primary MYC-responsive genes (83). A total of 98% of these genes were repressed, indicating that the direct effect of MYC regulation is transcriptional activation (83). OCT4 is one of the four pluripotency factors, the expression of which is sufficient to reprogram differentiated fibroblasts into induced pluripotent stem cells (84). However, the genes OCT4 regulates in pluripotent stem cells are difficult to identify, as the half-life of its protein and mRNA are much too long for traditional knockdown methods to isolate the primary effects of depletion (85). A recent study compared extended knockdown to rapid depletion with targeted protein degradation and found that only the latter was able to identify that the primary effect of OCT4 on transcription is the activation of pluripotency factors and that the delayed activation of trophoblast-associated genes is a secondary effect of OCT4 depletion (85). A key takeaway from these studies is that these factors directly activate transcription of their target genes. The growing list of transcription factors that can be acutely perturbed provides evidence that most factors do not activate some direct targets and repress others. Additionally, these findings highlight a recurring theme: in contrast to extended knockdown approaches, the acute depletion of

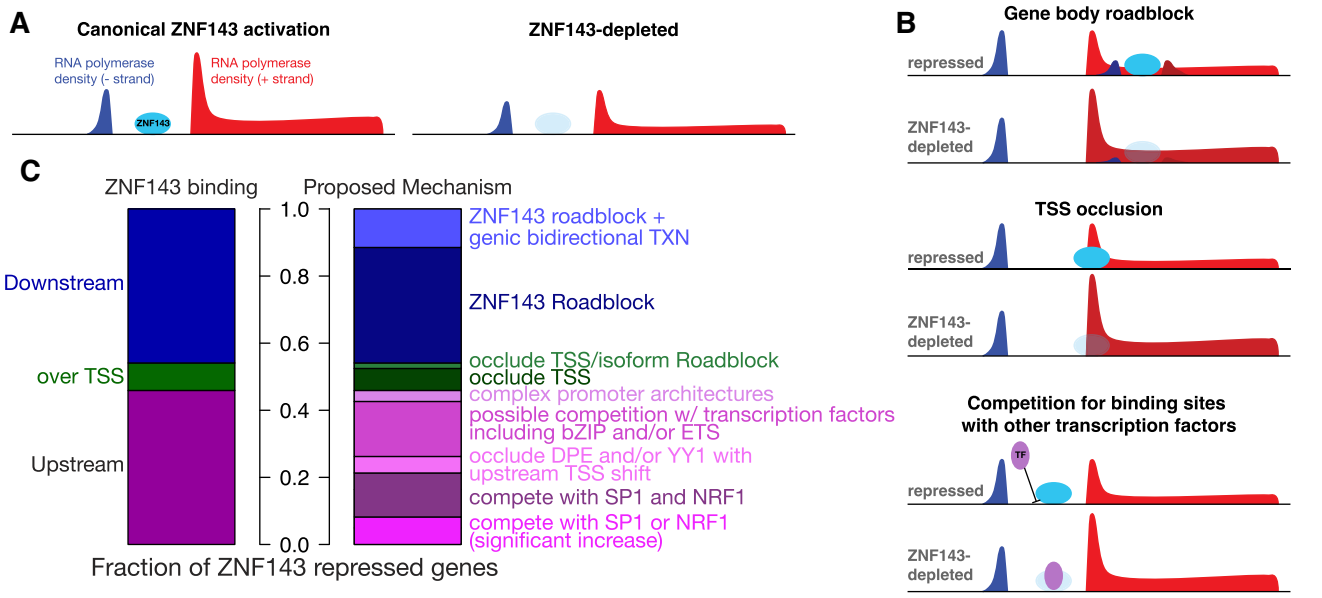

Figure 7. The molecular function of ZNF143 is to bind DNA and facilitate initiation. (**A**) ZNF143 binds to the promoter and stimulates transcription at the majority of its target genes. (**B**) ZNF143 binding can cause repression if binding occurs over a TSS, immediately downstream of a TSS or in competition with other activators. (**C**) ZNF143's repression mechanisms can be further specified depending on the local environment of the ZNF143 binding site. The number of genes in the left barchart from top to bottom is 28, 5 and 28. The right bar chart top to bottom has the following number of genes in each category: 7 (roadblock/bidirectional), 21 (roadblock), 1 (roadblock and TSS occlusion), 4 (TSS occlusion), 2 (complex promoters with no proposed mechanism), 10 (possible competition with sequence-specific promoter factors), 3 (occlude DPE and/or YY1), 8 (possible competition with SP1 and/or Nrf1) and 5 (competition with SP1 or Nrf1).

sequence-specific factors tends to impact the transcription of only a limited number of primary response genes (86,87).

There is substantial data suggesting that transcription factors specialize and recruit either corepressors or coactivators. We can conceive of exceptions to this rule, but we would argue that a factor can become a fundamentally different protein with distinct functions based on ligand binding status or post-translational modifications. The most well-characterized example of this is the thyroid hormone receptor (THR). THR binds to DNA and recruits corepressors in the absence of thyroid hormone (88); THR recruits coactivators when bound by thyroid hormone (89–92). Post-translational modifications, such as phosphorylation or acetylation, fundamentally change the identity of a protein and this may result in the ability to differentially interact with cofactors. Although we were unable to identify well-characterized examples of post-translational modifications that switch interaction partners from coactivators to corepressors or vice versa, this mechanism has been suggested for STAT3, which recruits corepressors exclusively when acetylated (93). Extending this general mechanism, a transcription factor may be bound to DNA, but only interact with coactivators when post-translationally modified. In the absence of the modification, the factor would be a functional repressor by occluding the binding sites of other activating factors and failing to recruit coactivators.

Another key part of context for defining the role of a TF is promoter strength. Transcription factor activity modeled in *E. coli* demonstrates that a TF can appear to change from an activator to repressor or vice versa depending on promoter strength and which step of the transcription cycle is regulated by the TF (94). In their model, transcription factors were characterized by their ability to either regulate the stability of RNA polymerase or promote transcription initiation. They found that TFs with strong stabilizing functions but weaker initiating abilities moved from activation to repression as promoter strength increased. We can envision how the same RNA polymerase stabilization mechanism might appear to repress transcription in the presence of a strong promoter if the stabilization interferes with the ability of RNA polymerase to begin transcription. On the other end of the spectrum, TFs that were strong initiators but weaker stabilizers moved from repression to activation with increasing promoter strength. Once again, we see that a TF appears to change activity when in reality the strong promoter may make it easier for transcription to initiate when perhaps other factors are able to improve RNA polymerase stability. The importance of promoter strength in eukaryotes is highlighted by an effector domain mutagenesis and mapping study that identified effector domains with the ability to seemingly both activate and repress transcription (95). Here the definition of 'activator' and 'repressor' becomes important, as this study defined activators as effector domains able to increase expression as compared to basal levels from a minimally active promoter and repressors as those able to decrease expression as compared to basal levels from a constitutively active promoter. According to these definitions, it is possible that a 'bifunctional' effector domain is actually a weak activator if it promotes transcription, but at a lower level than the constitutively active promoter. Although the details of transcription regulation in prokaryotes differs from eukaryotes, the overall principle appears to be similar in that promoter strength, combined with the particular role of a TF, both contribute to whether a particular TF appears to be activating or repressing transcription. Understanding the relationship between promoter strength and the specific functions of TFs can explain their seemingly dual role in activating and repressing gene expression.

Although this study convincingly demonstrates that ZNF143 depletion can lead to the repression of local genes

via our proposed plausible mechanisms (Figure 7), we have yet to distinguish between incidental regulation and conserved evolutionary mechanisms that specifically govern these genes. The identity of the ZNF143-repressed genes suggest some coordinated regulatory control. *FIS1* is a mitochondrial fission gene and ZNF143 positively regulates nuclearly encoded mitochondrial genes (24). We speculate that activating nuclearly encoded mitochondrial genes that are involved in mitochondrial biogenesis and function while simultaneously repressing fission genes can be a strategic response to enhance mitochondrial function and biogenesis. This coordinated response may build a robust mitochondrial network to meet increased metabolic demands or recover from damage more effectively. Another gene that is repressed in *cis* by ZNF143 is *THAP11*. *THAP11* binds to a nearly identical sequence motif as ZNF143 (14,96), although there is no clear evolutionary conservation of their respective DNA binding domains. The regulation of *THAP11* by ZNF143 is not clear from our data, although we propose that ZNF143 displaces an ETS factor (Supplementary Figure S8A). Regulation of *THAP11* is likely more complicated, as close inspection of the locus reveals an unannotated TSS that is flanked by two ZNF143 ChIP peaks, which are also likely THAP11 binding sites (Supplementary Figure S9). Moreover, usage of this unannotated TSS increases substantially upon ZNF143 degradation. Given the interplay between ZNF143 and the regulation of genes like *FIS1* and *THAP11*, it is likely that at least some aspects of regulatory repression are crucial for maintaining homeostasis and orchestrating cellular responses to metabolic changes. Although our study is within a single cell line, the molecular functions of transcription factors tend to be consistent across cell types, even though the specific genes that are regulated can be different.

This work underscores the significance of using rapidly inducible systems to study molecular mechanisms. Additionally, we highlight that while genomic experiments and analyses indicated ZNF143 was repressing a subset of genes in *cis*, a more detailed examination of these repressed genes was essential to suggest mechanisms of repression. We recognize that a thorough understanding of biological systems necessitates an in-depth grasp of the individual components and mechanisms. We therefore anticipate that the focus of scientific inquiry will shift away from broad molecular genomics studies, high throughput reporter assays and large scale screens towards more focused, mechanistic investigations.

Data availability

All analysis details and code are available at https://github.com/guertinlab/znf143_degron and https://doi.org/10.5281/zenodo.14080968. Raw sequencing files and processed bigWig files are available from GEO accession record GSE266491 (PRO-seq), GSE266490 (ATAC-seq) and GSE266489 (ChIP-seq). Quality control metrics and number of replicates for PRO-seq (Supplementary Figure S1), ChIP-seq (Supplementary Figure S3) and ATAC-seq (Supplementary Figure S4) exceed standards within the field.

Supplementary data

Supplementary Data are available at NAR Online.

Acknowledgements

We thank the Cold Spring Harbor Laboratory Gene Expression course participants of 2023: Rafiou Agoro, Anusha Bhatt, Nicole Brossier, Magda Bujnowska, Terri Cain, Frederic Carew, Mariano Colon-Caraballo, Nadia Côté, Elisa Gorostieta Salas, Rebecca Mello, Erik Rodriguez Teran, Sanket Shah, Jenny Shim, Tejus Sreelal, Bradley Stevens and Dejauwne Young; and 2024: Rio Barrere-Cain, Ellie Benitez, Kayleigh Biegler, Joe Brett, Arianna Cocco, Aja Coleman, Mikayla Eppert, Jérôme Gagneux, Raj Gaji, Cecilia Gavilan, Melody Hancock, MaryClaire Haseley, Peter Hoboth, Monica Mesa Perez, Quentin Phillips and Nivedhya Venas. The CSHL GeneX participants each generated a replicate of the ATAC-seq data under the direction of J.D., T.G.S. and M.J.G. This work was funded by R35-GM128635 awarded to MJG.

Author contributions: J.D., T.G.S., R.M. and M.J.G. analyzed the data. J.D., S.K.M., T.G.S. and M.J.G. performed the experiments. J.D., T.G.S. and M.J.G. conceptualized and developed the project. J.D., T.G.S. and M.J.G. wrote the manuscript.

Funding

Funding for open access charge: Center for Scientific Review [R35-GM128635 to MJG].

Conflict of interest statement

None declared.

References

1. Lewis,E. B. (1978) A gene complex controlling segmentation in *Drosophila*. *Nature*, **276**, 565–570.
2. Nüsslein-Volhard,C. and Wieschaus,E. (1980) Mutations affecting segment number and polarity in *Drosophila*. *Nature*, **287**, 795–801.
3. Duarte,F. M., Fuda,N. J., Mahat,D. B., Core,L. J., Guertin,M. J. and Lis,J. T. (2016) Transcription factors GAF and HSF act at distinct regulatory steps to modulate stress-induced gene activation. *Genes Dev.*, **30**, 1731–1746.
4. Scholes,C., DePace,A. H. and Sánchez,Á. (2017) Combinatorial gene regulation through kinetic control of the transcription cycle. *Cell Syst.*, **4**, 97–108.
5. Scott,T. G., Sathyan,K. M., Gioeli,D. and Guertin,M. J. (2024) TRPS1 modulates chromatin accessibility to regulate estrogen receptor alpha (ER) binding and ER target gene expression in luminal breast cancer cells. *PLoS Genet.*, **20**, e1011159.
6. Kumar,V., Green,S., Stack,G., Berry,M., Jin,J.-R. and Chambon,P. (1987) Functional domains of the human estrogen receptor. *Cell*, **51**, 941–951.
7. Kumar,V. and Chambon,P. (1988) The estrogen receptor binds tightly to its responsive element as a ligand-induced homodimer. *Cell*, **55**, 145–156.
8. Westwood,J. T., Clos,J. and Wu,C. (1991) Stress-induced oligomerization and chromosomal relocalization of heat-shock factor. *Nature*, **353**, 822–827.
9. Guertin,M., Petesch,S., Zobeck,K., Min,I. and Lis,J. (2010) *Drosophila* heat shock system as a general model to investigate transcriptional regulation. *Cold Spring Harb. Symp. Quant. Biol.*, **75**, 1–9.
10. Nishimura,K., Fukagawa,T., Takisawa,H., Kakimoto,T. and Kanemaki,M. (2009) An auxin-based degron system for the rapid depletion of proteins in nonplant cells. *Nat. Methods*, **6**, 917–922.

11. Nabet,B., Roberts,J. M., Buckley,D. L., Paulk,J., Dastjerdi,S., Yang,A., Leggett,A. L., Erb,M. A., Lawlor,M. A., Souza,A., *et al.* (2018) The dTAG system for immediate and target-specific protein degradation. *Nat. Chem. Biol.*, **14**, 431–441.
12. Nabet,B., Ferguson,F. M., Seong,B. K. A., Kuljanin,M., Leggett,A. L., Mohardt,M. L., Robichaud,A., Conway,A. S., Buckley,D. L., Mancias,J. D., *et al.* (2020) Rapid and direct control of target protein levels with VHL-recruiting dTAG molecules. *Nat. Commun*, **11**, 4687.
13. Schuster,C., Myslinski,E., Krol,A. and Carbon,P. (1995) Staf, a novel zinc finger protein that activates the RNA polymerase III promoter of the selenocysteine tRNA gene.. *EMBO J.*, **14**, 3777–3787.
14. Ngondo-Mbongo,R. P., Myslinski,E., Aster,J. C. and Carbon,P. (2013) Modulation of gene expression via overlapping binding sites exerted by ZNF143, Notch1 and THAP11. *Nucleic Acids Res.*, **41**, 4000–4014.
15. Guertin,M. J., Zhang,X., Coonrod,S. A. and Hager,G. L. (2014) Transient estrogen receptor binding and p300 redistribution support a squelching mechanism for estradiol-repressed genes. *Mol. Endocrinol.*, **28**, 1522–1533.
16. Schmidt,S. F., Larsen,B. D., Loft,A. and Mandrup,S. (2016) Cofactor squelching: Artifact or fact?. *Bioessays*, **38**, 618–626.
17. Schmidt,S. F., Larsen,B. D., Loft,A., Nielsen,R., Madsen,J. G. S. and Mandrup,S. (2015) Acute TNF-induced repression of cell identity genes is mediated by NFκB-directed redistribution of cofactors from super-enhancers. *Genome Res.*, **25**, 1281–1294.
18. Heidari,N., Phanstiel,D. H., He,C., Grubert,F., Jahanbani,F., Kasowski,M., Zhang,M. Q. and Snyder,M. P. (2014) Genome-wide map of regulatory interactions in the human genome. *Genome Res.*, **24**, 1905–1917.
19. Bailey,S. D., Zhang,X., Desai,K., Aid,M., Corradin,O., Cowper-Sal·lari,R., Akhtar-Zaidi,B., Scacheri,P. C., Haibe-Kains,B. and Lupien,M. (2015) ZNF143 provides sequence specificity to secure chromatin interactions at gene promoters. *Nat. Commun*, **6**, 6186.
20. Zhang,K., Li,N., Ainsworth,R. I. and Wang,W. (2016) Systematic identification of protein combinations mediating chromatin looping. *Nat. Commun*, **7**, 12249.
21. Yang,Y., Zhang,R., Singh,S. and Ma,J. (2017) Exploiting sequence-based features for predicting enhancer–promoter interactions. *Bioinformatics*, **33**, i252–i260.
22. Liu,S., Cao,Y., Cui,K., Tang,Q. and Zhao,K. (2022) Hi-TrAC reveals division of labor of transcription factors in organizing chromatin loops. *Nat. Commun*, **13**, 6679.
23. Zhang,M., Huang,H., Li,J. and Wu,Q. (2024) ZNF143 deletion alters enhancer/promoter looping and CTCF/cohesin geometry. *Cell Rep.*, **43**, 113663.
24. Magnitov,M. D., Maresca,M., Alonso Saiz,N., Teunissen,H., Braccioli,L. and de Wit,E. (2024) ZNF143 is a transcriptional regulator of nuclear-encoded mitochondrial genes that acts independently of looping and CTCF. bioRxiv doi: https://doi.org/10.1101/2024.03.08.583864, 12 March 2024, preprint: not peer reviewed.
25. Narducci,D. N. and Hansen,A. S. (2024) Putative looping factor ZNF143/ZFP143 is an essential transcriptional regulator with no looping function. bioRxiv doi: https://doi.org/10.1101/2024.03.08.583987, 12 March 2024, preprint: not peer reviewed.
26. Sathyan,K. M., Scott,T. G. and Guertin,M. J. (2020) ARF-AID: a rapidly inducible protein degradation system that preserves basal endogenous protein levels. *Curr. Protoc. Mol. Biol.*, **132**, e124.
27. Kent,W. J., Sugnet,C. W., Furey,T. S., Roskin,K. M., Pringle,T. H., Zahler,A. M. and Haussler,D. (2002) The human genome browser at UCSC. *Genome Res.*, **12**, 996–1006.
28. Grandi,F. C., Modi,H., Kampman,L. and Corces,M. R. (2022) Chromatin accessibility profiling by ATAC-seq. *Nat. Protoc.*, **17**, 1518–1552.
29. Langmead,B. and Salzberg,S. L. (2012) Fast gapped-read alignment with Bowtie 2. *Nat. Methods*, **9**, 357–359.
30. Li,H., Handsaker,B., Wysoker,A., Fennell,T., Ruan,J., Homer,N., Marth,G., Abecasis,G. and Durbin,R. (2009) The sequence alignment/map format and SAMtools. *Bioinformatics*, **25**, 2078–2079.
31. Martins,A. L., Walavalkar,N. M., Anderson,W. D., Zang,C. and Guertin,M. J. (2018) Universal correction of enzymatic sequence bias reveals molecular signatures of protein/DNA interactions. *Nucleic Acids Res.*, **46**, e9.
32. Zhang,Y., Liu,T., Meyer,C. A., Eeckhoute,J., Johnson,D. S., Bernstein,B. E., Nusbaum,C., Myers,R. M., Brown,M., Li,W., *et al.* (2008) Model-based analysis of ChIP-Seq (MACS). *Genome Biol.*, **9**, R137.
33. Love,M. I., Huber,W. and Anders,S. (2014) Moderated estimation of fold change and dispersion for RNA-seq data with DESeq2. *Genome Biol.*, **15**, 550.
34. Mahat,D. B., Kwak,H., Booth,G. T., Jonkers,I. H., Danko,C. G., Patel,R. K., Waters,C. T., Munson,K., Core,L. J., *et al.* (2016) Base-pair-resolution genome-wide mapping of active RNA polymerases using precision nuclear run-on (PRO-seq). *Nat. Protoc.*, **11**, 1455–1476.
35. Sathyan,K. M., McKenna,B. D., Anderson,W. D., Duarte,F. M., Core,L. and Guertin,M. J. (2019) An improved auxin-inducible degron system preserves native protein levels and enables rapid and specific protein depletion. *Genes Dev.*, **33**, 1441–1455.
36. Judd,J., Wojenski,L. A., Wainman,L. M., Tippens,N. D., Rice,E. J., Dziubek,A., Villafano,G. J., Wissink,E. M., Versluis,P., Bagepalli,L., *et al.* (2020) A rapid, sensitive, scalable method for Precision Run-On sequencing (PRO-seq). bioRxiv doi: https://doi.org/10.1101/2020.05.18.102277, 19 May 2020, preprint: not peer reviewed.
37. Scott,T. G., Martins,A. L. and Guertin,M. J. (2022) Processing and evaluating the quality of genome-wide nascent transcription profiling libraries. bioRxiv doi: https://doi.org/10.1101/2022.12.14.520463, 16 December 2022, preprint: not peer reviewed.
38. Martin,M. (2011) Cutadapt removes adapter sequences from high-throughput sequencing reads. *EMBnet J.*, **17**, 10–12.
39. Smith,J. P., Dutta,A. B., Sathyan,K. M., Guertin,M. J. and Sheffield,N. C. (2021) PEPPRO: quality control and processing of nascent RNA profiling data. *Genome Biol.*, **22**, 155.
40. Anderson,W. D., Duarte,F. M., Civelek,M. and Guertin,M. J. (2020) Defining data-driven primary transcript annotations with primaryTranscriptAnnotation in R. *Bioinformatics*, **36**, 2926–2928.
41. Kent,W. J., Zweig,A. S., Barber,G., Hinrichs,A. S. and Karolchik,D. (2010) BigWig and BigBed: enabling browsing of large distributed datasets. *Bioinformatics*, **26**, 2204–2207.
42. Wang,Z., Chu,T., Choate,L. A. and Danko,C. G. (2019) Identification of regulatory elements from nascent transcription using dREG. *Genome Res.*, **29**, 293–303.
43. Bailey,T. L., Johnson,J., Grant,C. E. and Noble,W. S. (2015) The MEME suite. *Nucleic Acids Res.*, **43**, W39–W49.
44. Dutta,A. B., Lank,D. S., Przanowska,R. K., Przanowski,P., Wang,L., Nguyen,B., Walavalkar,N. M., Duarte,F. M. and Guertin,M. J. (2023) Kinetic networks identify TWIST2 as a key regulatory node in adipogenesis. *Genome Res.*, **33**, 314–331.
45. Hoops,S., Sahle,S., Gauges,R., Lee,C., Pahle,J., Simus,N., Singhal,M., Xu,L., Mendes,P. and Kummer,U. (2006) COPASI—a complex pathway simulator. *Bioinformatics*, **22**, 3067–3074.
46. Zimmer,J. T., Rosa-Mercado,N. A., Canzio,D., Steitz,J. A. and Simon,M. D. (2021) STL-seq reveals pause-release and termination kinetics for promoter-proximal paused RNA polymerase II transcripts. *Mol. Cell*, **81**, 4398–4412.
47. Larson,D. R., Zenklusen,D., Wu,B., Chao,J. A. and Singer,R. H. (2011) Real-time observation of transcription initiation and elongation on an endogenous yeast gene. *Science*, **332**, 475–478.
48. Gressel,S., Schwalb,B. and Cramer,P. (2019) The pause-initiation limit restricts transcription activation in human cells. *Nat. Commun*, **10**, 3603.

49. Jonkers,I. and Lis,J. T. (2015) Getting up to speed with transcription elongation by RNA polymerase II. *Nat. Rev. Mol. Cell Biol.*, **16**, 167–177.
50. Bailey,T. L. (2021) STREME: accurate and versatile sequence motif discovery. *Bioinformatics*, **37**, 2834–2840.
51. Bailey,T. L. and Gribskov,M. (1998) Combining evidence using p-values: application to sequence homology searches.. *Bioinformatics*, **14**, 48–54.
52. Stuart,E. A., King,G., Imai,K. and Ho,D. (2011) MatchIt: nonparametric preprocessing for parametric causal inference. *J. Stat. Softw.*, **42**, 1–28.
53. Jindal,G. A., Bantle,A. T., Solvason,J. J., Grudzien,J. L., D'Antonio-Chronowska,A., Lim,F., Le,S. H., Song,B. P., Ragsac,M. F., Klie,A., *et al.* (2023) Single-nucleotide variants within heart enhancers increase binding affinity and disrupt heart development. *Dev. Cell*, **58**, 2206–2216.
54. Lim,F., Solvason,J. J., Ryan,G. E., Le,S. H., Jindal,G. A., Steffen,P., Jandu,S. K. and Farley,E. K. (2024) Affinity-optimizing enhancer variants disrupt development. *Nature*, **626**, 151–159.
55. Kwak,H., Fuda,N. J., Core,L. J. and Lis,J. T. (2013) Precise maps of RNA polymerase reveal how promoters direct initiation and pausing. *Science*, **339**, 950–953.
56. Reddy,T. E., Pauli,F., Sprouse,R. O., Neff,N. F., Newberry,K. M., Garabedian,M. J. and Myers,R. M. (2009) Genomic determination of the glucocorticoid response reveals unexpected mechanisms of gene regulation. *Genome Res.*, **19**, 2163–2171.
57. Guertin,M. J. and Lis,J. T. (2010) Chromatin landscape dictates HSF binding to target DNA elements. *PLoS Genet.*, **6**, e1001114.
58. Hasterok,S., Scott,T. G., Roller,D. G., Spencer,A., Dutta,A. B., Sathyan,K. M., Frigo,D. E., Guertin,M. J. and Gioeli,D. (2023) The androgen receptor does not directly regulate the transcription of DNA damage response genes. *Mol. Cancer Res.*, **21**, 1329–1341.
59. Fuda,N. J., Ardehali,M. B. F. and Lis,J. T. (2009) Defining mechanisms that regulate RNA polymerase II transcription in vivo. *Nature*, **461**, 186–192.
60. Wagner,E. J., Tong,L. and Adelman,K. (2023) Integrator is a global promoter-proximal termination complex. *Mol. Cell*, **83**, 416–427.
61. Santana,J. F., Collins,G. S., Parida,M., Luse,D. S. and Price,D. H. (2022) Differential dependencies of human RNA polymerase II promoters on TBP, TAF1, TFIIB and XPB. *Nucleic Acids Res.*, **50**, 9127–9148.
62. Luse,D. S., Parida,M., Spector,B. M., Nilson,K. A. and Price,D. H. (2020) A unified view of the sequence and functional organization of the human RNA polymerase II promoter. *Nucleic Acids Res.*, **48**, 7767–7785.
63. Core,L. J., Waterfall,J. J. and Lis,J. T. (2008) Nascent RNA sequencing reveals widespread pausing and divergent initiation at human promoters. *Science*, **322**, 1845–1848.
64. Core,L. J., Martins,A. L., Danko,C. G., Waters,C. T., Siepel,A. and Lis,J. T. (2014) Analysis of nascent RNA identifies a unified architecture of initiation regions at mammalian promoters and enhancers. *Nat. Genet.*, **46**, 1311–1320.
65. Azofeifa,J. G. and Dowell,R. D. (2017) A generative model for the behavior of RNA polymerase. *Bioinformatics*, **33**, 227–234.
66. Burke,T. W. and Kadonaga,J. T. (1997) The downstream core promoter element, DPE, is conserved from *Drosophila* to humans and is recognized by TAFII60 of *Drosophila*. *Genes Dev.*, **11**, 3020–3031.
67. Seto,E., Shi,Y. and Shenk,T. (1991) YY1 is an initiator sequence-binding protein that directs and activates transcription in vitro. *Nature*, **354**, 241–245.
68. Athanikar,J. N., Badge,R. M. and Moran,J. V. (2004) A YY1-binding site is required for accurate human LINE-1 transcription initiation. *Nucleic Acids Res.*, **32**, 3846–3855.
69. Benner,C., Konovalov,S., Mackintosh,C., Hutt,K. R., Stunnenberg,R. and Garcia-Bassets,I. (2013) Decoding a signature-based model of transcription cofactor recruitment dictated by cardinal cis-regulatory elements in proximal promoter regions. *PLoS Genet.*, **9**, e1003906.
70. Dudnyk,K., Cai,D., Shi,C., Xu,J. and Zhou,J. (2024) Sequence basis of transcription initiation in the human genome. *Science*, **384**, eadj0116.
71. Grant,C. E., Bailey,T. L. and Noble,W. S. (2011) FIMO: scanning for occurrences of a given motif. *Bioinformatics*, **27**, 1017–1018.
72. Gill,G., Pascal,E., Tseng,Z. H. and Tjian,R. (1994) A glutamine-rich hydrophobic patch in transcription factor Sp1 contacts the dTAFII110 component of the *Drosophila* TFIID complex and mediates transcriptional activation. *Proc. Natl Acad. Sci. U.S.A.*, **91**, 192–196.
73. McKnight,S. L. and Kingsbury,R. (1982) Transcriptional control signals of a eukaryotic protein-coding gene. *Science*, **217**, 316–324.
74. Jones,T., Sigauke,R. F., Sanford,L., Taatjes,D. J., Allen,M. A. and Dowell,R. D. (2024) A transcription factor (TF) inference method that broadly measures TF activity and identifies mechanistically distinct TF networks. bioRxiv doi: https://doi.org/10.1101/2024.03.15.585303, 16 March 2024, preprint: not peer reviewed.
75. Ptashne,M. (2004) In: *A genetic switch: phage lambda revisited*.
76. Johnson,A. D., Meyer,B. J. and Ptashne,M. (1979) Interactions between DNA-bound repressors govern regulation by the λ phage repressor. *Proc. Natl Acad. Sci. U.S.A.*, **76**, 5061–5065.
77. Meyer,B. J., Maurer,R. and Ptashne,M. (1980) Gene regulation at the right operator (OR) of bacteriophage λ: II. OR1, OR2, and OR3: their roles in mediating the effects of repressor and cro. *J, Mol. Biol.*, **139**, 163–194.
78. Lin,C. Y., Lovén,J., Rahl,P. B., Paranal,R. M., Burge,C. B., Bradner,J. E., Lee,T. I. and Young,R. A. (2012) Transcriptional amplification in tumor cells with elevated c-Myc. *Cell*, **151**, 56–67.
79. Nie,Z., Hu,G., Wei,G., Cui,K., Yamane,A., Resch,W., Wang,R., Green,D. R., Tessarollo,L., Casellas,R., *et al.* (2012) c-Myc is a universal amplifier of expressed genes in lymphocytes and embryonic stem cells. *Cell*, **151**, 68–79.
80. Sabo,A., Kress,T. R., Pelizzola,M., De Pretis,S., Gorski,M. M., Tesi,A., Morelli,M. J., Bora,P., Doni,M., Verrecchia,A., *et al.* (2014) Selective transcriptional regulation by Myc in cellular growth control and lymphomagenesis. *Nature*, **511**, 488–492.
81. Walz,S., Lorenzin,F., Morton,J., Wiese,K. E., von Eyss,B., Herold,S., Rycak,L., Dumay-Odelot,H., Karim,S., Bartkuhn,M., *et al.* (2014) Activation and repression by oncogenic MYC shape tumour-specific gene expression profiles. *Nature*, **511**, 483–487.
82. Lorenzin,F., Benary,U., Baluapuri,A., Walz,S., Jung,L. A., von Eyss,B., Kisker,C., Wolf,J., Eilers,M. and Wolf,E. (2016) Different promoter affinities account for specificity in MYC-dependent gene regulation. *elife*, **5**, e15161.
83. Muhar,M., Ebert,A., Neumann,T., Umkehrer,C., Jude,J., Wieshofer,C., Rescheneder,P., Lipp,J. J., Herzog,V. A., Reichholf,B., *et al.* (2018) SLAM-seq defines direct gene-regulatory functions of the BRD4-MYC axis. *Science*, **360**, 800–805.
84. Takahashi,K. and Yamanaka,S. (2006) Induction of pluripotent stem cells from mouse embryonic and adult fibroblast cultures by defined factors. *cell*, **126**, 663–676.
85. Bates,L. E., Alves,M. R. and Silva,J. C. (2021) Auxin-degron system identifies immediate mechanisms of OCT4. *Stem Cell Rep.*, **16**, 1818–1831.
86. Sheppard,H. E., Dall'Agnese,A., Park,W. D., Shamim,M. H., Dubrulle,J., Johnson,H. L., Stossi,F., Cogswell,P., Sommer,J., Levy,J., *et al.* (2021) Targeted brachyury degradation disrupts a highly specific autoregulatory program controlling chordoma cell identity. *Cell Rep. Med.*, **2**, 100188.
87. Stengel,K. R., Ellis,J. D., Spielman,C. L., Bomber,M. L. and Hiebert,S. W. (2021) Definition of a small core transcriptional circuit regulated by AML1-ETO. *Mol. Cell*, **81**, 530–545.
88. Hörlein,A. J., Näär,A. M., Heinzel,T., Torchia,J., Gloss,B., Kurokawa,R., Ryan,A., Kamei,Y., Söderström,M., Glass,C. K. and et,al. (1995) Ligand-independent repression by the thyroid hormone receptor mediated by a nuclear receptor co-repressor. *Nature*, **377**, 397–404.

89. Grøntved,L., Waterfall,J. J., Kim,D. W., Baek,S., Sung,M.-H., Zhao,L., Park,J. W., Nielsen,R., Walker,R. L., Zhu,Y. J., *et al.* (2015) Transcriptional activation by the thyroid hormone receptor through ligand-dependent receptor recruitment and chromatin remodelling. *Nat. Commun*, **6**, 7048.
90. Lin,B. C., Hong,S.-H., Krig,S., Yoh,S. M. and Privalsky,M. L. (1997) A conformational switch in nuclear hormone receptors is involved in coupling hormone binding to corepressor release. *Mol. Cell. Biol.*, **17**, 6131–6138.
91. Fondell,J. D., Ge,H. and Roeder,R. G. (1996) Ligand induction of a transcriptionally active thyroid hormone receptor coactivator complex.. *Proc. Natl Acad. Sci. U.S.A.*, **93**, 8329–8333.
92. Chen,H., Lin,R. J., Schiltz,R. L., Chakravarti,D., Nash,A., Nagy,L., Privalsky,M. L., Nakatani,Y. and Evans,R. M. (1997) Nuclear receptor coactivator ACTR is a novel histone acetyltransferase and forms a multimeric activation complex with P/CAF and CBP/p300. *Cell*, **90**, 569–580.
93. Gambi,G., Di Simone,E., Basso,V., Ricci,L., Wang,R., Verma,A., Elemento,O., Ponzoni,M., Inghirami,G., Icardi,L., *et al.* (2019) The transcriptional regulator Sin3A contributes to the oncogenic potential of STAT3. *Cancer Res.*, **79**, 3076–3087.
94. Ali,M. Z., Guharajan,S., Parisutham,V. and Brewster,R. C. (2023) Regulatory properties of transcription factors with diverse mechanistic function. bioRxiv doi: https://doi.org/10.1101/2023.06.15.545127, 15 June 2023, preprint: not peer reviewed.
95. DelRosso,N., Tycko,J., Suzuki,P., Andrews,C., Aradhana,Mukund A., Liongson,I., Ludwig,C., Spees,K., Fordyce,P., *et al.* (2023) Large-scale mapping and mutagenesis of human transcriptional effector domains. *Nature*, **616**, 365–372.
96. Vinckevicius,A., Parker,J. B. and Chakravarti,D. (2015) Genomic determinants of THAP11/ZNF143/HCFC1 complex recruitment to chromatin. *Mol. Cell. Biol.*, **35**, 4135–4146.

Received: May 29, 2024. **Revised:** September 30, 2024. **Editorial Decision:** November 1, 2024. **Accepted:** November 20, 2024